ACADEMIA ROMÂNĂ
Revue Roumaine de Chimie
http://web.icf.ro/rrch/

Rev. Roum. Chim.,
2017, *62*(12), 947-955

NUMERICAL MODELING FOR SIMULATION AND EXPERIMENTAL INVESTIGATION ON PURIFICATION PROCESS OF TDI BY ZONE MELTING

Kun ZHOU,[a,b*] Yueyong YAN,[a] Lianying AN,[a,b] Ke WANG[a] and Tao WANG[b]

[a] College of Materials and Chemistry & Chemical Engineering, Chengdu University of Technology, Chengdu 610059, China
[b] Mineral Resources Chemistry Key Laboratory of Sichuan Higher Education Institutions, Chengdu University of Technology, Chengdu 610059, China

Received February 13, 2017

A method of zone melting was applied to measure the effective distribution coefficient of the impurity 2, 6-toluene diisocyanate under different conditions, using a purity of 80% toluene diisocyanate (i.e. TDI-80) as the raw material. The influence of zone melting rate, temperature difference between the molten zone, zone melting passes on the concentration distribution of impurity was analyzed, and the numerical model of the impurity 2,6-toluene diisocyanate distribution was established. The results show that the zone melting can effectively separate the two TDI isomers; zone melting rate and the temperature difference between the molten zone are the main parameters affecting the effective distribution coefficient of impurity; the numercial model can satisfy the experimental values well, through comparison of experimental and the calculated values, and it can be better to indicate the concentration distribution of 2,6-toluene diisocyanate after several zone melting passes; finally the model can provide a theoretical guidance on the purification process of TDI by zone melting.

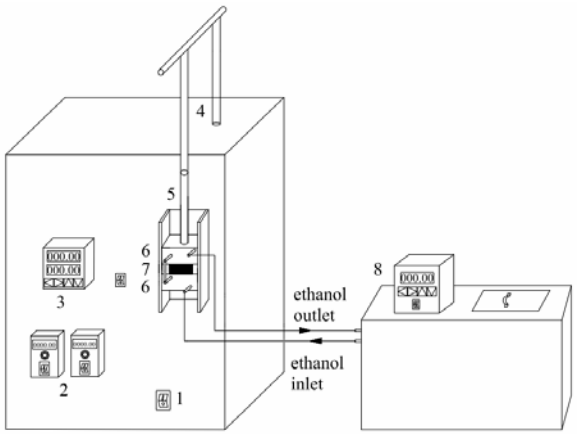

INTRODUCTION

Toluene diisocyanate, also named TDI, has two isomeric compounds: 2, 4-tolylene diisocyanate (2, 4-TDI) and 2, 6-toluene diisocyanate (2, 6-TDI). And it is easy to react with the compounds containing active hydrogen atoms or hydroxyl to produce urea, amino acid, polyurethane, etc. TDI is one of the most important raw materials for polyurethane industry; its application and development are more under and more attention by the world chemical industry. The most important use of TDI is for organic synthesis, production of foamed plastics and it can also be used for the production of soft foams, elastomers, paints, coatings, adhesives and other. With the rapid development of polyurethane industry, the demand for TDI is increasing rapidly in China. By the end of 2012, China's TDI production capacity has reached 790,000 tons, becoming the world's biggest producer and consumer of polyurethane. In addition, according to the content of 2, 4-TDI in the product, the industrial TDI is divided into TDI-65, TDI-80 and TDI-100 three kinds of different specifications of products. However the added value of TDI-100 is the highest; the current market price of TDI-100 is about 6,000 dollars per ton, and it is about 2 times higher than the two other products. Therefore, it has very practical significance for the purification of industrial TDI.

At present, the main production processes of TDI-100 has: phosgenation method; pressure crystallization; atmospheric pressure crystallization; catalyst polymerization method; adsorption separation

* Corresponding author: kunzhou925@163.com

method. The method above belongs to the chemical method, is a phosgenation method and a catalyst polymerization method. However, its technological process is complicated, the raw material consumption is large, the side reaction is excessive, the reaction rate is low, and the energy consumption is large. At present, the liquid chlorine and phosgene used in the production process of TDI are highly toxic products, and they will cause serious pollution to the environment. Pressure crystallization; atmospheric pressure crystallization and adsorption separation method belong to the physical production method, but these methods have the disadvantages of low product purity and high production cost. Nevertheless, the purification method by zone melting has some advantages, such as high yield, good purification effect, and it can produce high purity, even super pure materials, like cadmium, [1] copper, indium, tellurium,[2] 1-naphthol, phosphoric acid[3] and so on. Its outstanding advantage is that the purified material does not have any contact with other solvents or chemicals.[4] In addition, in crystal growth, the crystal size and optical quality can be significantly improved by zone melting technology.[5-7] Besides, some research shows that zone melting is a viable method for purification process of water[8] and Au/Ge alloy.[9] And it is also called green technology, [10] because of its low energy consumption, no pollution. So far, there is no literature report on the purification process of TDI by zone melting. In this paper, TDI-80 is used as raw material, purified by zone melting technology, and then the experimental verification is carried out on the basis of the establishment of the mathematical model.

EXPERIMENTAL

Materials and Experimental Apparatus

Raw material TDI ($C_9H_6N_2O_2$, molecular mass 174.15, Figure 1) was purchased from Guangzhou Da-hua Group Co. Ltd., its brand is TDI-80. And it was prepared by recrystallization in the laboratory. After suspension crystallization, the mass fraction of TDI, measured by GC, is 90.1 %. The more detailed information of TDI used in the study is shown in Table 1. A laboratory scale intermittent zone melting equipment for purifying TDI was established by a laboratory team independently as shown in Figure 2.

Experimental Process

The raw material is added to a 10×200 mm quartz glass tube, then the glass tube is placed in the ice water bath to be solidified. The driving motor connected to the glass tube by the mobile unit is carried out at a certain rate of zone melting, thus the molten zone can be determined by a certain rate through the whole sample bar. After the completion of the first zone melting, the driving device will quickly return to the beginning of the quartz glass tube, and then the second zone melting will be carried out. The temperature of the heater is controlled by a digital display regulator; the temperature of the upper and lower ends of the cooler is controlled by an external super low temperature constant temperature tank, and the refrigerant used in the experiment is industrial alcohol. The content of 2, 6-TDI in the sample was analyzed by gas chromatography. The chromatography column was an AT. XE-60 with the size 30 m ×0.25 mm ×0.25 μm. And the chromatography column temperature was 150 ºC; the temperature of vaporizing chamber was 250 ºC. The hydrogen flame ionization detector was selected, and its temperature was 250 ºC. The carrier gas was high purity nitrogen and its flow rate was 1.0 mL/min, and injection volume was 0.15 μL.

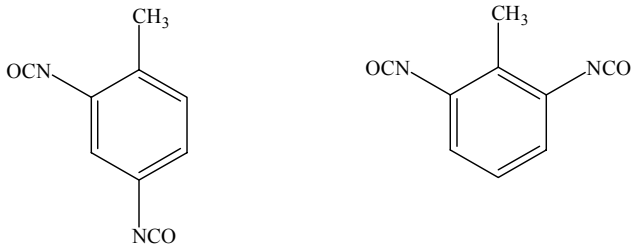

2,4-TDI 2,6-TDI

Fig. 1 – Chemical structure of two isomers of TDI.

Table 1

Detailed Information of Materials Used in the Study

Chemical name	Source	Initial mass fraction purity	Purification method	Final mass fraction purity	Analysis method
tolylene diisocyanate	Guangzhou Da-hua Group Co. Ltd.	80.0	suspension crystallization	90.1	GC[a]

[a]Gas-liquid chromatography.

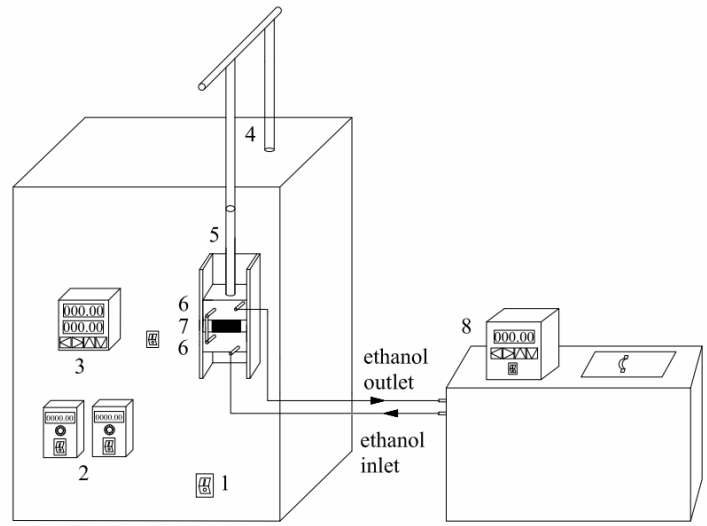

Fig. 2 – Schematic diagram of experimental apparatus of zone melting
1. Power source, 2. Velocity controller, 3. Temperature controller, 4. Ingot holder, 5. Quartz glass tube, 6. Cooling jackets, 7. Heater, 8. Low temperature thermostatic bath.

NUMERICAL MODELING

The zone melting method was first proposed and used as a method of separation and purification by Pfann.[11] The principle of zone melting is shown in Figure 3. When the molten zone was slowly passed through the sample bar with uniform distribution of impurity, the concentration distribution of impurity in the sample is different, and the zone melting technology is the use of this segregation phenomenon, so as to achieve the effect of purification. As shown in Figure 3, the molten zone was moved from one end of the sample to the other in the process of the zone melting. After that, the impurity will be divided into one side of sample bar depending on the values of the effective distribution coefficient k_{eff} and the initial concentration of impurity in sample bar C_0. The effective distribution coefficient k_{eff} of impurity was defined by Prasad and Munirathnam.[12] And for $k_{\text{eff}} < 1$, the impurity was gathered at the right end of the sample bar, while for $k_{\text{eff}} > 1$, the impurity was gathered at the left side of the sample bar. Impurity having k_{eff} values close to 1 are difficult to segregate.

The distribution of the impurity along the sample bar for one and multiple zone melting passes will be evaluated by considering the following assumptions:

(1) The k_{eff} is constant in the whole process of zone melting.

(2) Molten zone length, zone melting rate, and cross-sectional area of molten zone are constant of each pass.

(3) The densities of solid and liquid are the same.

(4) Diffusion of the impurity in the solid is negligible.

(5) Diffusion of the impurity in the liquid is complete.

(6) The solidification interface is planar, and in a state of equilibrium.

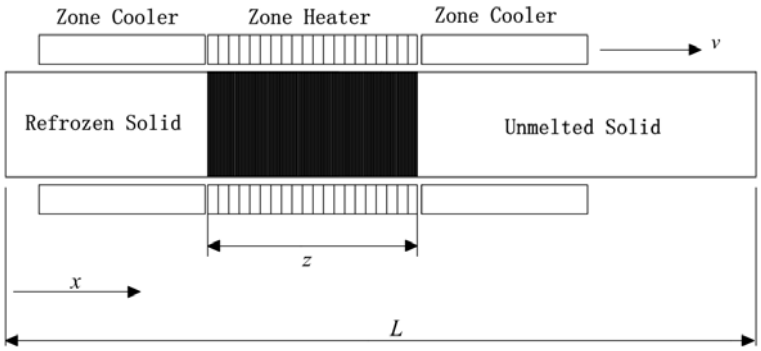

Fig. 3 – Schematic diagram of the principle of zone melting.

Concentration Distribution after One Molten Zone Pass

After the end of one zone melting pass, the concentration distribution of impurity in the sample bar except for the last molten zone can be expressed by the following Pfann's equation.

$$\frac{C_{S,1}(x)}{C_0} = 1-(1-k_{eff})e^{\frac{-k_{eff}x}{z}} \quad (0 \le x \le 1-z) \quad (1)$$

In the last molten zone of sample bar, the Scheil's equation can be used to express the concentration distribution of impurity of normal freezing.[13]

$$\frac{C_{S,1}(x)}{C_0} = \left\{1-(1-k_{eff})e^{\frac{-k_{eff}(1-x)}{z}}\right\} \times \left\{1-\frac{[x-(1-z)]}{z}\right\}^{k_{eff}-1} \quad (1-z < x \le 1) \quad (2)$$

Concentration Distribution after Multiple Molten Zone Passes

There is a gradient of the impurity concentration distribution along the sample bar after one molten zone pass. To obtain the numerical modeling after multiple molten zone passes, the sample bar will consider four different regions: x=0, 0<x≤1-z, 1-z<x<1, x=1. Yabing Q. *et al.*[14] and Yongsheng R. *et al.*[15] have developed a numerical model of impurity distribution of multiple passes respectively. And the following models are based on Ghosh,[16] Spim's[17] model and can be considered as an expanded application in the purification process of TDI by zone melting.

(1) x=0 For the initial position of sample bar, the impurity in the first molten zone is totally mixed after multiple molten zone passes, and the concentration of impurity in any position of the molten zone is the same. Thus, the total impurity mass in the first molten zone can be written as $z.C_{L,n}(0)$. If the first molten zone is divided into m infinitesimal elements of width dx, the total impurity mass also can be expressed as Eq. (3).

$$z \cdot C_{L,n}(0) = \mathrm{d}x\left[\sum_{i=1}^{m-1} C_{S,n}(x_i)\right] \quad (3)$$

(3) 1-z<x<1 In the last molten zone, the molten zone is gradually reduced and the sample was normal freezing because there is no more new impurity entering the molten zone. The average concentration of the impurity in the last molten zone can be expressed as Eq. (9).

$$\overline{C_{S,n}(x)} = \frac{C_0 - \int_0^{1-z} C_{S,n}(x)\mathrm{d}x}{z} \quad (9)$$

And k_{eff}=$C_{S,n}(x)$/$C_{L,n}(x)$, So Eq. (3) can be rewritten as Eq. (4).

$$\frac{C_{S,n}(x)}{C_0} = \left(\frac{k_{eff}\cdot \mathrm{d}x}{z}\right)\cdot\left[\sum_{i=0}^{m-1}\frac{C_{S,n-1}(x_i)}{C_0}\right] \quad (4)$$

(2) 0<x≤1-z In this region, the molten zone for each moving dx distance, the impurity in the solid phase and the molten zone can reach a balance. The variation of the impurity in the molten zone is $z(\triangle C_L)$, and the variation of impurity at the point dx is dx($\triangle C_S$). According to the mass conservation, the variation of impurity in the molten zone is equal to the variation of the impurity at the point dx. Thus, it can be expressed as Eq. (5).

$$z(\Delta C_L) = \mathrm{d}x(\Delta C_S) \quad (5)$$

Here, $\triangle C_L$ and $\triangle C_S$ can be expressed as follow equations.

$$\Delta C_L = \frac{C_{S,n}}{k_{eff}} \quad (6)$$

$$\Delta C_S = C_{S,n-1}(x+z-\mathrm{d}x) - C_{S,n}(x-\mathrm{d}x) \quad (7)$$

Hence, the concentration distribution of the impurity in this region is given by Eq. (8)

$$\frac{C_{S,n}(x)}{C_0} = \frac{C_{S,n}(x-\mathrm{d}x)}{C_0} + \left(\frac{k_{eff}\cdot \mathrm{d}x}{z}\right)\cdot\left[\frac{C_{S,n-1}(x+z-\mathrm{d}x) - C_{S,n}(x-\mathrm{d}x)}{C_0}\right] \quad (8)$$

$$\int_0^{1-z} C_{S,n}(x)\mathrm{d}x = \left[\sum_{i=1}^{m-1} C_{S,n}(x_i)\right]\mathrm{d}x \quad (10)$$

The equation (9) and (10) are brought into the Scheil's equation to derive the concentration distribution of the impurity in this region.

$$\frac{C_{S,n}(x)}{C_0} = k_{\text{eff}}(1-x)^{k_{\text{eff}}-1} \cdot (z^{-k_{\text{eff}}}) \cdot \left\{ \frac{C_0 - \sum_{i=1}^{m-1} C_{S,n}(x_i) \cdot \mathrm{d}x}{C_0} \right\} \tag{11}$$

(4) x=1 For the impurity in the whole sample bar, the total amount of impurity can be expressed as Eq. (12) by applying mass conservation.

$$\int_0^1 C_{S,n}(x)\mathrm{d}x = C_0 \tag{12}$$

$$\int_0^1 C_{S,n}(x)\mathrm{d}x = \left[\sum_{i=1}^{R-1} C_{S,n}(x_i) \right] \mathrm{d}x + C_{S,n}(1) \cdot \mathrm{d}x \tag{13}$$

Therefore, the concentration of the impurity at the point x=1 is given by Eq. (14)

$$\frac{C_{S,n}(1)}{C_0} = R - \sum_{i=1}^{R-1} \frac{C_{S,n}(x_i)}{C_0} \tag{14}$$

RESULTS AND DISCUSSION

The effective distribution coefficient of the impurity 2, 6-TDI under different conditions is shown in Table 2. According to the effective distribution coefficient under different conditions and the concentration of impurity 2, 6-TDI in different position, the relative concentration C_S/C_0 of 2, 6-TDI is used as the vertical coordinate, the value of the distance x is used as the horizontal coordinate, and the experimental results are compared with the mathematical model, and the mathematical model is verified by the experimental data.

Effect of Zone Melting Temperature Difference

The effect of zone melting temperature difference on 2, 6-TDI concentration distribution is shown in Figure 4. From Figure 4, it can be concluded that the theoretical and experimental values of C_S/C_0 in the first half of the sample bar are in good agreement. When x>0.8, the distance between the experimental value and the theoretical value is gradually increased. Secondly, at the starting end of the sample bar the theoretical values and experimental values are small, and the values of C_S/C_0 gradually increases with the increasing of x, so a large amount of 2, 6-TDI is enriched at the end of the sample bar. This shows that the two isomers can be separated under a certain condition, and it also means that TDI can be purified by zone melting. Finally, according to Figure 4, it is obvious to find that with the increasing of zone melting temperature, the concentration of 2, 6-TDI shows a different degree of reduction at the front end of sample bar, however when the x>0.9 is just the opposite.

The effect of zone melting temperature difference on $C_{S,n}(x)$ value is mainly through affecting the effective distribution coefficient of 2,6-TDI. When the zone melting rate, the number of zone passes, and zone length are constant, the values of $C_{S,n}(x)$ will be changed at the difference of temperature. The greater the melting temperature difference is, the greater the effect of the diffusion of the molecules on the crystalline interface and in the molten zone, which is beneficial to the diffusion of molecules. Thus, the greater the mass transfer driving force between the crystalline interface and the molten zone, the greater the mass change of the impurity in the solid-liquid phase and the values of C_S/C_0 are more far away from 1. In addition, when the sample is solidified on the crystalline interface, the larger zone melting temperature difference can reduce the probability of the formation of the high and low crystalline interface phenomenon, and this phenomenon will affect the distribution of the impurity in the solid-liquid phase, which will affect the effective distribution coefficient of the impurity. Therefore, in the case of certain conditions, the greater the zone melting temperatures difference in a certain range, the better the purification effect.

Table 2

The effective distribution coefficient of impurity 2, 6-TDI under different conditions

Temperature difference, ºC	Zone melting rate *v*, mm/h				
	10	15	20	25	30
40	0.290	0.478	0.668	0.724	0.910
45	0.262	0.379	0.477	0.618	0.772
50	0.186	0.315	0.418	0.588	0.715

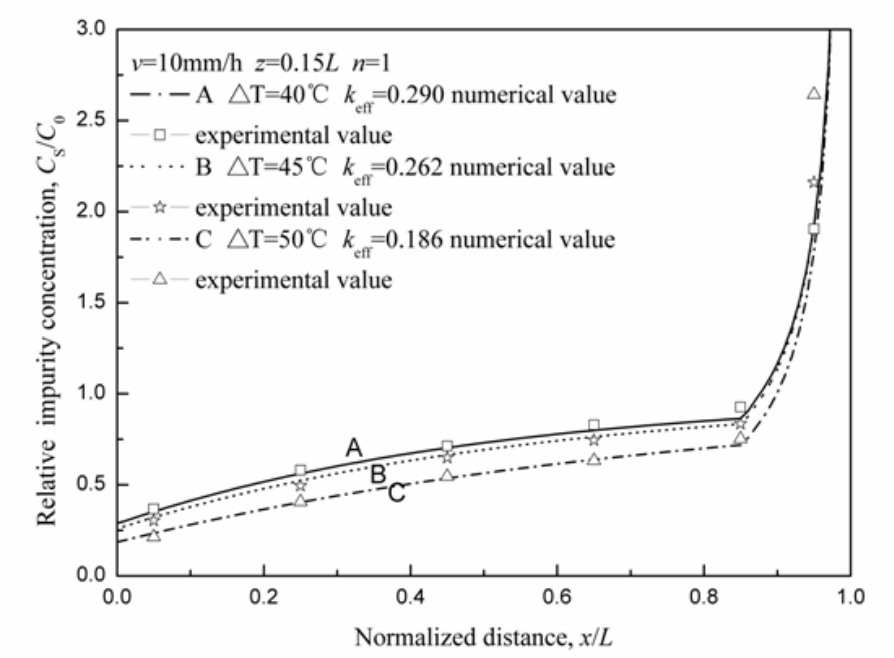

Fig. 4 – The comparison of temperature difference between experimental and numerical value.

Effect of Zone Melting Rate

The zone melting rate is an important factor affecting the purification effect under certain conditions. From Figure 5, it can be concluded that the calculated values of C_S/C_0 show good agreement with the experimental values. And the impurity concentration on the starting end of the melting tube is less than the initial concentration of the sample, while the end is higher than the initial concentration, so the concentration of 2, 6-TDI is gradually increasing from the beginning to the end of the whole sample bar. Besides, according to Figure 5, when the zone melting rate increases, the concentration of 2, 6-TDI at the starting end of the sample bar increases, but the concentration decreases at the end of sample bar. At the same position of the front end of the zone melting tube, the concentration of the impurity 2, 6-TDI decreases with the decrease of zone melting rate.

The influence of zone melting rate on concentration distribution of 2, 6-TDI in the zone melting tube is mainly by affecting the effective distribution coefficient. It takes time to transfer between the molten zone and the crystalline interface, and reach the equilibrium distribution for the solute. If the zone melting rate is too fast, it will affect the concentration distribution of the solute, because it doesn't have enough time to reach the equilibrium in the solid-liquid phase. According to the above analysis, the smaller the zone melting rate, the more favorable the purification process under the other conditions unchanged. However, in practical applications, the zone melting rate is smaller, and the time required for one zone melting pass is increased, so taking into account the efficiency and other issues, the zone melting rate should not be too small.

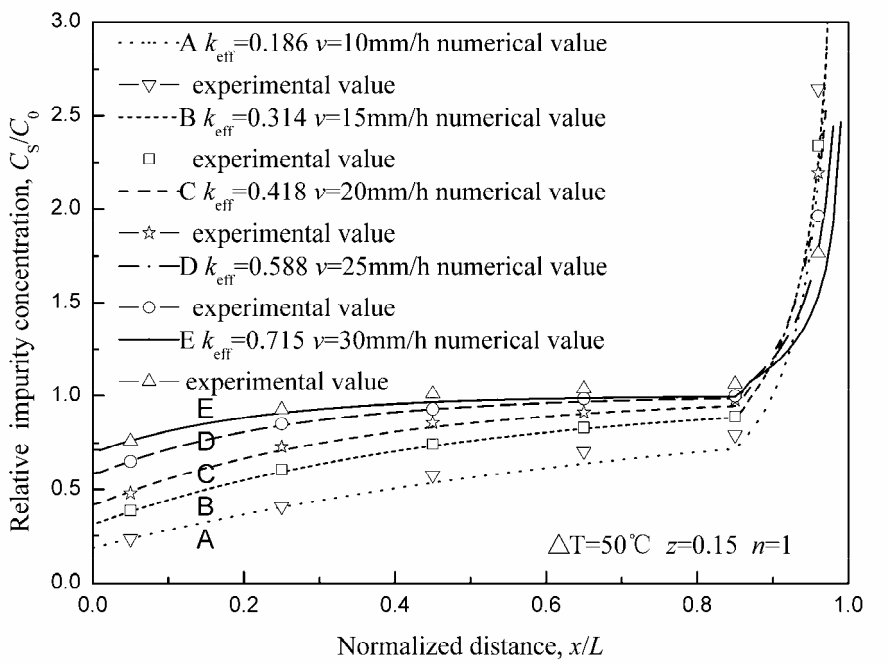

Fig. 5 – The comparison of zone melting rate between experimental and numerical value.

Effect of Zone Melting Passing Times

For the zone melting, the increase of zone melting times, that is, the increase of a redistribution process of the solute, the solute can be constantly transferred from the solid phase to the liquid phase, so as to achieve the purpose of purification. The influence of number of zone melting passes on zone melting purification process is shown in Figure 6. As shown in Figure 6, with the increase of number of zone melting passes, the difference between theoretical and experimental values of the same position $C_{S,n}(x)$ is gradually increasing. This is due to the experimental process has not reached the theoretical equilibrium distribution. In addition, in a certain range of x, the same position after multiple zone melting, the theoretical and experimental values of $C_{S,n}(x)$, are gradually reduced, and at the close to the end position is the opposite. It is obvious that when the number of the theoretical zone melting is 4 times, nearly 75% of the sample in the quartz glass tube has reached the purity of TDI-100; however the number of the actual zone melting is far more than this.

Effect of Molten Zone Length

The change of molten zone length has no effect on the effective distribution coefficient of impurity, but the different lengths of molten zone can contain a different content of impurity, therefore, different lengths of the molten zone have a very important influence on the concentration distribution of impurity. For the effect of molten zone length on the 2, 6-TDI distribution, the area of $C_S/C_0<1$ is mainly considered. Because the effective distribution coefficient of 2, 6-TDI is less than 1, the starting end of the sample bar is a purified area. When the value of C_S/C_0 is smaller, the purified region is longer after zone melting, which shows that the purification effect of the zone melting method is better. Figure 7 shows the concentration distribution of impurity 2, 6-TDI in different molten zone length (a: 1 pass; b: 5 passes; c: 10 passes; d: 15 passes). From Figure 7a, the zone melting effect is getting better and better with the increase of the molten zone length after one pass. After 5 passes, the zone melting effect of z=0.1L is the best (Figure 6b). However, when the number of zone melting passes reached 10 or 15 passes, it was found that with the decrease of molten zone length, the zone melting effect is getting better and better (Figure 7c, d). According to Figure 7a, b, c, d, it shows that with the increase of zone melting passes, the molten zone of z=0.05L curve gradually close to the horizontal axis, and the change of z=0.05L curve is very small after 15 passes. It's obvious that the previous few zone melting passes are prone to adopt the longer molten zone length, and the shorter length of molten zone should be adopted in multiple zone melting passes in the process of zone melting.

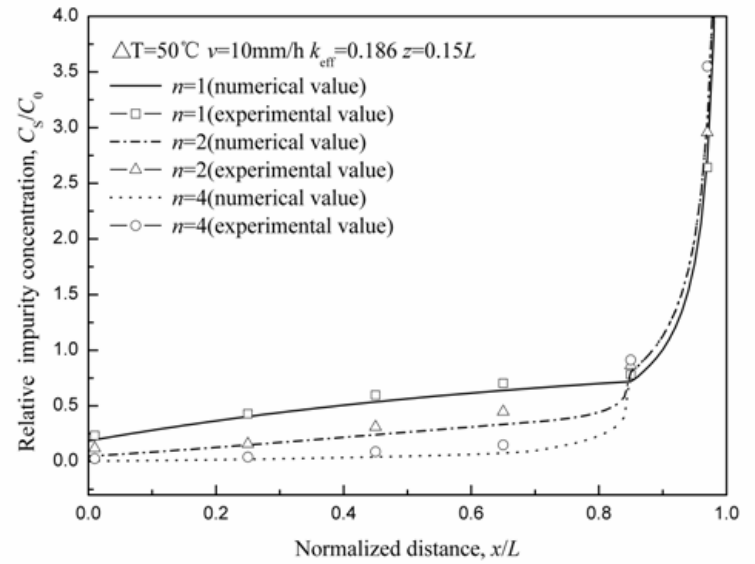

Fig. 6 – The comparison of zone passing times between experimental and numerical value.

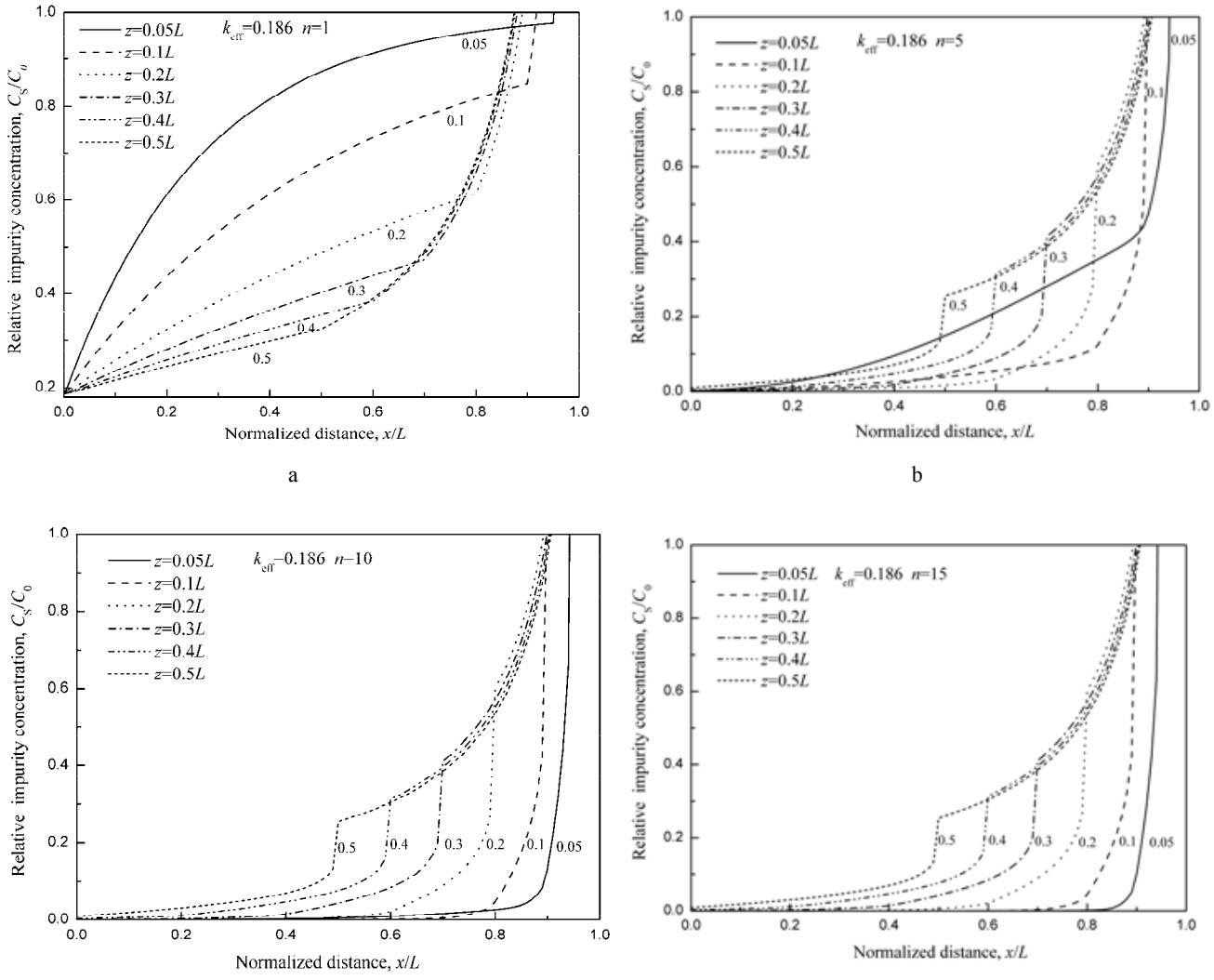

Fig. 7 – Concentration distribution of impurity 2, 6-TDI with different molten zone lengths.
Zone melting passing times: a, n = 1; b, n = 5; c, n = 10; d, n = 15.

CONCLUSION

The crucial points are as follows: (1) In this paper, the purification process of TDI by zone melting was studied, and numerical model was established for predicting the concentration distribution of impurity 2, 6-TDI after multiple purification process of zone melting, which can provide a theoretical guide for the purification of TDI-100 by zone melting method. (2) Under certain conditions, the zone melting method can effectively separate the two isomers (2, 4-TDI and 2, 6-TDI). The main factors that affect the purification effect are the effective distribution coefficient k_{eff}, the number of zone melting passes n, and the molten zone length z. (3) The effective distribution coefficient of impurity 2, 6-TDI is mainly affected by zone melting rate and zone melting temperature difference.

Nomenclature

z length of molten zone, mm
L total length of sample bar, mm
v molten zone velocity, mm/h
x distance along the sample bar, mm
n number of zone melting passes
m number of width dx in the one molten zone
R number of width dx in the whole sample bar
k_{eff} effective distribution coefficient
C_0 initial concentration of 2,6-TDI, mg.g^{-1}
C_S concentration of 2,6-TDI in solid, mg.g^{-1}
C_L concentration of 2,6-TDI in liquid, mg.g^{-1}
ΔC_L variation of the concentration of 2,6-TDI in molten zone after the distance of the molten zone moving dx
ΔC_S variation of the concentration of 2,6-TDI in solid phase after the distance of the molten zone moving dx
$C_{S,n}(x)$ concentration of 2,6-TDI in solid phase at x point after n-th pass, mg.g^{-1}
$C_{L,n}(x)$ concentration of 2,6-TDI in liquid phase at x point after n-th pass, mg.g^{-1}
$\overline{C_{S,n}(x)}$ average concentration of 2,6-TDI in last molten zone after n-th pass, mg.g^{-1}

REFERENCES

1. N. R. Munirathnam, D. S. Prasad, C. Sudheer, J. V. Rao and T. L. Prakash, *B. Mater. Sci.*, **2005**, *28*, 209-212.
2. N. R. Munirathnam, D. S. Prasad, C. Sudheer and T. L. Prakash, *J. Cryst. Growth,* **2003**, *254*, 262-266.
3. Y. S. Ren and X. X. Duan, *Can. J. Chem. Eng.*, **2013**, *91*, 318-323.
4. J. M. Prausnitz, R. N. Lichtenthaler and E. G. D. Azevedo, "Molecular Thermodynamics of Fluid-Phase Equilibria", Pearson Education, 1998.
5. S. Mariko, T. Akiko, S. Misaki, S. Yukihiro and O. Tohru, *Langmuir,* **2013**, *29*, 9668-9676.
6. Y. S. Chung, N. Shin, J. Kang, Y, Jo, V. M. Prabhy, S. K. Satija, R. J. Kline, D. M. Delongchamp, M. F. Toney, M. A. Loth, B. Purushothaman, J. E. Anthony and D. Y. Yoon, *J. Am. Chem. Soc.,* **2011**, *133*, 412-415.
7. K. W. Yeh, C. T. Ke, T. W. Huang, T. K. Chen, Y. L. Huang, P. M. Wu and M. K. Wu, *Cryst. Growth Des.*, **2009**, *9*, 4847-4851.
8. J. Oughton, *J. Chem. Edu.*, **2001**, *78*, 1373-1374.
9. Q. Liu, R. Zou, J. Wu, K. Xu, A. Liu, Y. Bando, D. Golberg and J. Hu, *Nano Lett.*, **2015**, *15*, 2809-2816.
10. J. Ulrich, *Cryst. Growth Des.*, **2004**, *4*, 879-880.
11. W. G. Pfann, *Trans. AIME*, **1952**, *194*, 747-536.
12. D. S. Prasad and N. R. Munirathnam, *Int. J. Mod. Phys. B,* **2008**, *22*, 2583-2588.
13. E. Scheil, *Z. Metallkd.,* **1942**, *34*, 70-72.
14. Y. Qi, J. Li, B. Wang, K. Zhou, J. Luo, C. Ye and X. Jia, *J. Chem. Eng. JPN.,* **2012**, *45*, 571-576.
15. Y. Ren, X. Duan, B. Wang, M. Huang and J. Li, *Ind. Eng. Chem. Res.,* **2012**, *51*, 4035-4040.
16. K. Ghosh, V. N. Mani and S. Dhar, *Tetrahedron*, **1993**, *49*, 6229-6234.
17. J. A. Spim, M. J. S. Bernadou and A. Garcia, *J. Alloy. Compd.,* **2000**, *298*, 299-305.